JOURNAL OF THERMOPHYSICS AND HEAT TRANSFER
Vol. 13, No. 1, January–March 1999

Analysis of Supercritical Startup Behavior for Cryogenic Heat Pipes

Y. H. Yan* and J. M. Ochterbeck†
Clemson University, Clemson, South Carolina 29634

A theoretical analysis was conducted to describe the startup process from the supercritical state for axially grooved cryogenic heat pipes. Using an approximation method, a heat-balance integral solution was developed to predict the rewetting velocity, liquid front position, and transient axial temperature distributions for axially grooved cryogenic heat pipes. The developed model assumes an initially uniform axial temperature distribution and divides the startup process into two characteristic regions, based on whether a liquid column is established in the condenser region. The predicted transient temperature profiles of two cryogenic oxygen heat pipes were in good agreement with previous experimental microgravity flight data.

Nomenclature

A = coefficient defined in Eq. (12)
A_f = cross-sectional area of the working fluid
A_l = cross-sectional area of the liquid channel
A_s = cross-sectional area of the heat-pipe wall
B = coefficient defined in Eq. (12)
C_e = effective heat capacity
c = specific heat
D = coefficient defined in Eq. (12)
D_h = hydraulic diameter
E = thermal energy
F = force
h = groove thickness
h_{fg} = latent heat of liquid–vapor phase change
k = thermal conductivity
L_a = length of adiabatic section
L_c = length of condenser
L_e = length of evaporator
P = internal pressure
P_c = critical pressure
P_r = reduced pressure
R = gas constant
Re = Reynolds number
r = capillary radius
T = temperature
T_c = critical temperature
T_{cond} = condenser temperature
T_r = reduced temperature
T_0 = initial temperature
t = time
U = liquid mean velocity
U_r = liquid rewetting velocity
v = specific volume of vapor
w = groove width
z = compressibility factor
α_e = effective heat diffusivity
β = coefficient defined in Eq. (3)
δ = penetration depth
ε = liquid layer length
θ = temperature difference
θ_D = Debye temperature
μ = viscosity
ρ = density
τ_w = wall friction

Subscripts
cap = capillary
f = working fluid
frict = friction
l = liquid
s = heat-pipe wall

Received Oct. 13, 1997; revision received Aug. 14, 1998; accepted for publication Aug. 17, 1998.

*Graduate Research Assistant, Mechanical Engineering Department.

†Assistant Professor, Mechanical Engineering Department. E-mail: jay.ochterbeck@ces.clemson.edu. Senior Member AIAA.

Introduction

THE most severe transients that potentially result in heat-pipe failure generally occur during the initial startup of a heat pipe in thermal equilibrium with the environment, as the working fluid is initially quiescent. Depending on the thermal environment and the corresponding working fluid state, heat-pipe startup can be classified into three separate categories: 1) normal, 2) supercritical, and 3) frozen. In heat pipes for cryogenic applications, a gaseous or supercritical state prevails for the working fluids, e.g., hydrogen, nitrogen, oxygen, at room-temperature conditions. During startup, the heat pipe must be cooled until the fluid temperature is below the critical point temperature. The startup process requires condensation of the working fluid and wetting of the wicking structure before the heat pipe becomes operational.

Previous examinations of supercritical startup have been conducted using numerical models and have presented good basic information regarding the transient supercritical startup characteristics. Investigations of supercritical startup for cryogenic heat pipes in the past have been generally conducted using finite difference numerical analysis[1] or by startup limits associated with restart failure.[2] Although these investigations have provided insight into issues of supercritical startup, overall analytical tools for supercritical startup remain limited.

Related to the problem of wetting of the wicking structure, investigations have been conducted to examine the rewetting characteristics of finite length grooved plates with uniform heating and wall superheat to determine the transient response time for evaporator rewetting.[3–5] These analyses have confirmed several apparent characteristics of rewetting:

1) Increasing either the wall superheat or the heat input rate will decrease the rewetting velocity.

2) When no heat addition is applied, the liquid channel will reprime for any initial value of wall superheat, although at a decreasing rate for increasing superheat levels.

3) A heat input value exists such that the rewetting velocity may become equal to zero, i.e., the liquid supply rate is equal to the vaporization rate and the advancing column stagnates.

This investigation expands upon previous work using integral methods and closed-form solutions for the rewetting of a finite length grooved plate with uniform heating and wall superheat, and applies them to the issue of supercritical startup for cryogenic heat pipes. Analytical solutions are presented and have compared favorably with experimental data for the startup characteristics of two axially grooved cryogenic heat pipes flown onboard the Space Shuttle. With the integral solutions, the rewetting velocities and axial temperature distributions of the cryogenic heat pipe can be determined throughout startup.

Analysis

The startup process of an axially grooved heat pipe initially at a uniform temperature T_0 is considered, where the initial temperature of the heat pipe is assumed to be greater than the critical point value. During startup, the condenser is cooled by a cryocooler, whereas the adiabatic section and evaporator are cooled by axial heat conduction to the condenser. When the temperature and pressure of the vapor decrease to levels below the critical-point values, the vapor begins to condense. After the condenser groove becomes filled with liquid, a liquid film from the condenser, driven by surface tension, will advance along the liquid channel.

During the period when a liquid column has been established, and because the dry region is at an elevated temperature, some of the liquid at the leading edge of the liquid front is vaporized and the remaining liquid advances with a rewetting velocity U_r, which is less than the mean film velocity U. Heat required to vaporize the liquid is supplied by heat conduction from the dry region. If the heat supplied from the dry region exceeds that required to vaporize all of the advancing liquid, then rewetting would not occur and the liquid film will recede. In the condenser, the liquid temperature is assumed to be uniform and equal to the wall temperature as given by the cryocooler temperature. It is important to note that although a temperature boundary condition is utilized to allow direct comparison with existing experimental data, the model easily can be adapted to utilize a heat-flux boundary condition. Other assumptions for the following analysis were made:

1) The heat conduction is one dimensional.

2) The fluid temperature is equal to the adjacent wall temperature and the fluid pressure is uniform.

3) The heat transfer between the heat pipe and the surroundings is negligible, although if known, any parasitic heat leaks or applied heat loads can be included as an input heat flux.

4) The thermal conductivity of the working fluid is negligible compared with the thermal conductivity of the heat-pipe wall.

Because of symmetry, a segment, or single axial groove, of the heat pipe was studied. The section was made through the axes of two adjacent fins, with such a segment shown schematically in Fig. 1.

The transient, axial heat conduction equation for the heat-pipe wall and wick structure is given by

$$\frac{\partial}{\partial x}\left(kA_s \frac{\partial T}{\partial x}\right) = (\rho_s A_s c_s + \rho_f A_f c_f)\frac{\partial T}{\partial t} \tag{1}$$

where the specific heat of the heat pipe wall can be expressed as a function of temperature[6]

$$c_s = 9R\left(\frac{T}{\theta_D}\right)^3 \int_0^{(\theta_D/T)} \frac{x^4 e^x}{(e^x - 1)^2}\,dx \tag{2}$$

The specific heat of the working fluid is a function of temperature and specific volume. Because the temperature and specific volume of the working fluid vary axially and temporarily, the specific heat is a very complicated function of time and axial position. For simplicity, the heat capacity of the working fluid was incorporated by adding a constant coefficient to the heat capacity of the heat-pipe wall. This coefficient was defined as

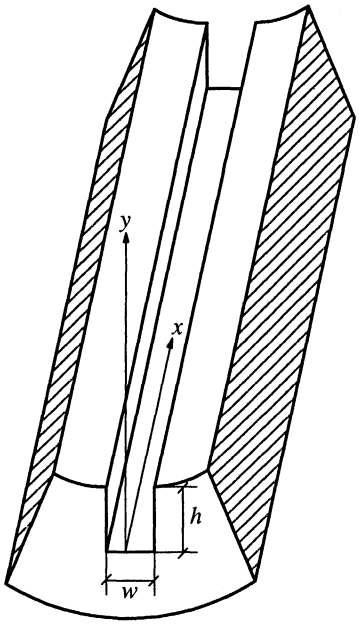

Fig. 1 Schematic of the modeled heat-pipe segment.

$$\beta = (\Delta E_s + \Delta E_f)/\Delta E_s \tag{3}$$

where ΔE_s and ΔE_f are the total internal energy change from the initial state to the final state for the heat-pipe wall and the working fluid, respectively. Using this assumption, Eq. (1) can be simplified as

$$\frac{\partial}{\partial x}\left(k\frac{\partial T}{\partial x}\right) = C_e \frac{\partial T}{\partial t} \tag{4}$$

where C_e is defined as

$$C_e = (1 + \beta)\rho_s c_s \tag{5}$$

The boundary condition in the condenser can be described as either a specified heat flux or a specified temperature. In this investigation, the case with specified temperature was examined. The analysis for a specified heat flux boundary condition can be obtained in a similar manner. Because the temperature in the condenser is assumed uniform, the origin of the coordinate system was selected to be located at the intersection between the condenser and the adiabatic section (Fig. 2). Thus, the boundary condition at the condenser end can be described as

$$T|_{x=0} = T_{\text{cond}} \tag{6}$$

As the vapor inside the heat pipe does not condense until the temperature and pressure are lower than the critical temperature and pressure, the startup process is divided into two stages. In the first stage, the vapor temperature or pressure is higher than the critical temperature or pressure, and the heat pipe is cooled only by pure heat conduction. In the second stage, the vapor temperature and pressure are lower than the critical temperature and pressure, and the heat pipe is cooled by conducting heat to the advancing liquid front. Based on this consideration, the analysis is separated into two segments.

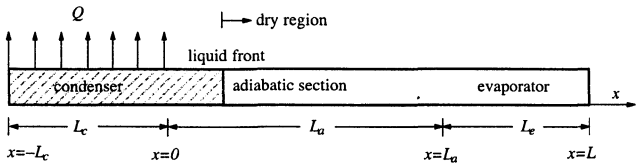

Fig. 2 Coordinate system used in modeling of the cryogenic heat-pipe startup process.

Stage 1: $T_{cond} > T_c$ or $P > P_c$

Because the primary mechanism of heat transfer in this stage is diffusion, the cooling effect resulting from the condenser heat rejection is not immediately propagated throughout the heat pipe, but is confined to a region extending from the condenser $x = 0$ to some penetration depth $x = \delta(t)$, where $\delta(t)$ is less than L. Beyond $\delta(t)$, the temperature gradient is zero and the temperature in this region is uniform. Therefore, this stage can be further divided into two parts with $\delta < L$ and $\delta = L$.

Penetration Depth Less than Heat Pipe Length $\delta < L$

The resulting governing equation and boundary conditions for this portion of the startup process are

$$\frac{\partial}{\partial x}\left(k\frac{\partial\theta}{\partial x}\right) = C_e\frac{\partial\theta}{\partial t} \tag{7}$$

$$\theta|_{x=0} = \theta_{cond} \tag{8}$$

$$\theta|_{x=\delta} = 0 \tag{9}$$

$$\left.\frac{\partial\theta}{\partial x}\right|_{x=\delta} = 0 \tag{10}$$

where $\theta = T - T_0$. Equation (9) indicates that the temperature at the penetration depth is equal to the initial temperature, whereas Eq. (10) specifies that the temperature gradient at the penetration depth, $x = \delta$, is zero. The solution to the set of Eqs. (7–10) was obtained using an integral method. Integrating the governing equation from $x = 0$ to $x = \delta$ yields

$$-k\left.\frac{\partial\theta}{\partial x}\right|_{x=0} = C_e\frac{\partial}{\partial t}\left(\int_0^\delta \theta\,dx\right) \tag{11}$$

Assuming a parabolic temperature profile

$$\theta = A + Bx + Dx^2 \tag{12}$$

and substituting Eqs. (8–10) into Eq. (12) yields the definition for the coefficients A, B, and D as

$$A = \theta_{cond}, \qquad B = -(2\theta_{cond}/\delta), \qquad D = \theta_{cond}/\delta^2 \tag{13}$$

Substituting Eq. (13) into Eq. (12) yields the expression for the temperature profile as

$$\theta = \theta_{cond} - \frac{2\theta_{cond}x}{\delta} + \frac{\theta_{cond}x^2}{\delta^2} = \theta_{cond}\left(1 - \frac{x}{\delta}\right)^2 \tag{14}$$

Substituting Eq. (14) into Eq. (11) provides a description of the time rate of change of the penetration depth

$$\frac{d\delta}{dt} = \frac{6\alpha_e}{\delta} - \frac{\delta}{\theta_{cond}}\frac{d\theta_{cond}}{dt} \tag{15}$$

where α_e is defined as

$$\alpha_e = k/C_e \tag{16}$$

In Eq. (15), the only unknown is the penetration depth δ. After δ is obtained by integrating Eq. (15) numerically, the temperature profile can be obtained using Eq. (14).

Once the axial temperature profile is known at a given time step, the internal pressure can be obtained from the thermodynamic relation

$$P = zRT/v \tag{17}$$

The compressibility factor z in Eq. (17) can be expressed as a function of reduced temperature and reduced specific volume[7]

$$z = z(T_r, v_r) = z_0(T_r, v_r) + \omega z_1(T_r, v_r) \tag{18}$$

where

$$T_r = T/T_c \tag{19}$$

$$v_r = vP_c/RT_c \tag{20}$$

Detailed information for the calculation of the compressibility factor is found in any thermodynamic text.[7]

Penetration Depth Equals Heat Pipe Length, $\delta = L$

At this point, the cooling effect of the condenser has propagated over the entire heat-pipe length, and the governing equation and boundary conditions are given by

$$\frac{\partial}{\partial x}\left(k\frac{\partial\theta}{\partial x}\right) = C_e\frac{\partial\theta}{\partial t} \tag{21}$$

$$\theta|_{x=0} = \theta_{cond} \tag{22}$$

$$\left.\frac{\partial\theta}{\partial x}\right|_{x=L} = 0 \tag{23}$$

Integrating Eq. (21) from $x = 0$ to $x = L$ yields

$$-\alpha_e\left.\frac{\partial\theta}{\partial x}\right|_{x=0} = \frac{\partial}{\partial t}\left(\int_0^L \theta\,dx\right) \tag{24}$$

Again, assuming a parabolic temperature profile

$$\theta = A + Bx + Dx^2 \tag{25}$$

and substituting Eqs. (22) and (23) into Eq. (25), yields the new definitions for coefficients A and B as

$$A = \theta_{cond}, \qquad B = -2DL \tag{26}$$

Substituting Eq. (26) into Eq. (25) yields an expression of the temperature profile as a function of the coefficient D

$$\theta = \theta_{cond} - 2DLx + Dx^2 \tag{27}$$

The time rate change of the coefficient D is obtained by substituting Eq. (27) into Eq. (24)

$$\frac{dD}{dt} = \frac{3}{2L^2}\left(\frac{d\theta_{cond}}{dt} - 2\alpha_e D\right) \tag{28}$$

In Eq. (28), the only unknown, D, can be numerically obtained by integrating Eq. (28), whereas the temperature profile can be obtained from Eq. (27). After the axial temperature profile was determined, the internal pressure is estimated in the same manner as described for the condition $\delta < L$.

Stage 2: $T_{cond} < T_c$ and $P < P_c$

When the condenser temperature is lower than the critical temperature and the internal pressure is lower than the critical pressure, the vapor begins to condense in the condenser section. The rewetting process was modeled as the rewetting of a rectangular groove. The advancing liquid layer is subjected to a capillary driving force that is induced by surface tension and opposed by the wall shear stress. The total liquid layer was taken as the control volume, and the liquid film advances at an average velocity that will vary with respect to the length of the liquid layer.[5] The momentum equation for the control volume therefore is given by

$$F_{cap} - F_{frict} = \frac{d(mU)}{dt} \tag{29}$$

or

$$\frac{2\sigma hw}{r} - \tau_w \varepsilon(2h + w) = hw \frac{d(\rho U\varepsilon)}{dt} \tag{30}$$

where the two terms on the left side of Eq. (30) represent the capillary force and the wall friction, respectively, and the right side of Eq. (30) represents the change of momentum.

Assuming that the liquid flow is laminar and Newtonian, the wall shear stress can be approximated as

$$\tau_w = \frac{\rho U^2}{2}\frac{16}{Re} = \frac{8\mu U}{D_h} = \frac{2\mu U(2h + w)}{hw} \tag{31}$$

The capillary radius r for a rectangular groove is given as[8]

$$r = w \tag{32}$$

Substituting Eqs. (31) and (32) into Eq. (30) yields the relationship

$$\frac{2\sigma h}{w} - \frac{2U\varepsilon}{h}\left(\frac{2h + w}{w}\right)^2 \mu = \rho h \frac{d(U\varepsilon)}{dt} \tag{33}$$

The associated initial condition for the advancing liquid column is given by

$$t = 0, \qquad \varepsilon = 0 \tag{34}$$

and the solution to Eq. (33) was determined as

$$U\varepsilon = \frac{\sigma h^2}{w[(2h + w)/w]^2\mu}\left(1 - \exp\left\{-\frac{2[(2h + w)/w]^2\mu t}{\rho h^2}\right\}\right) \tag{35}$$

Equation (35) represents an expression for U as a function of the liquid layer length and the rewetting time for an unheated rectangular groove. Because the velocity and position of the liquid column are related by

$$U = \frac{d\varepsilon}{dt} \tag{36}$$

then Eq. (35) can be expressed in the form

$$\varepsilon\frac{d\varepsilon}{dt} = \frac{\sigma h^2}{w[(2h + w)/w]^2\mu}\left(1 - \exp\left\{-\frac{2[(2h + w)/w]^2\mu t}{\rho h^2}\right\}\right) \tag{37}$$

Solving Eq. (37) with the initial condition provided by Eq. (34) yields

$$\varepsilon = \left(\frac{2\sigma h^2}{w[(2h + w)/w]^2\mu}\right)^{1/2}\left(t + \frac{\rho h^2}{2[(2h + w)/w]^2\mu} \times \left\{\exp\left[\frac{-2\mu t}{\rho h^2}\left(\frac{2h + w}{w}\right)^2\right] - 1\right\}\right)^{1/2} \tag{38}$$

If the length of the liquid layer is less than the length of the condenser, $\varepsilon < L_c$, the rewetting process is restricted to the condenser. The heat conduction in the region between $x = 0$ and $x = L$ is not affected by rewetting, i.e., the heat transfer process within the heat pipe remains pure heat conduction. The wall temperature was calculated using the same procedure as described in the previous section with the condition $\delta < L$.

When the liquid front reaches the interface between the condenser and the adiabatic section, $\varepsilon = L_c$, two possible cases exist. If the liquid mean velocity in the condenser is not sufficient to provide cooling to the dry region, the liquid front will stagnate and will not advance immediately. Thus, the wall temperature in the dry region remains independent of the rewetting. With increasing time, the liquid mean velocity in the condenser increases, because the liquid temperature continues to decrease with time, which results in the surface tension increasing and, thus, increasing the capillary driving force. Additionally, the heat flux from $x = 0^+$ to the condenser decreases and the latent heat of vaporization increases. Thus, the liquid front eventually will advance again. The heat transfer problem in this stage can be described as

$$\frac{\partial}{\partial x}\left(k\frac{\partial\theta}{\partial x}\right) = C_e\frac{\partial\theta}{\partial t} \tag{39}$$

$$\theta|_{x=\varepsilon-L_c} = \theta_{cond} \tag{40}$$

$$\left.\frac{\partial\theta}{\partial x}\right|_{x=L} = 0 \tag{41}$$

$$kA_s\left.\frac{\partial\theta}{\partial x}\right|_{x=\varepsilon-L_c} = \rho_l A_l h_{fg}\left(U - \frac{d\varepsilon}{dt}\right) \tag{42}$$

where Eq. (40) indicates that the liquid layer temperature equals the condenser temperature, and Eq. (42) represents the thermal energy transmitted across the liquid front line that is removed by liquid evaporation.

Assuming again a parabolic temperature profile

$$\theta = A + Bx + Dx^2 \tag{43}$$

and following the same procedure as outlined for the condition $\delta < L$, the temperature profile can be expressed as

$$\theta = \theta_{cond} - 2DL(x - \varepsilon + L_c) + D[x^2 - (\varepsilon - L_c)^2] \tag{44}$$

Integrating Eq. (39) from $x = \varepsilon - L_c$ to $x = L$ yields the time rate change of the coefficient D as

$$\frac{dD}{dt} = \frac{3}{2(L - \varepsilon + L_c)^2} \times \left[-2\alpha_e D + 2D(L - \varepsilon + L_c)\frac{d\varepsilon}{dt} - \frac{\theta_{cond}}{L - \varepsilon + L_c}\frac{d\varepsilon}{dt} + \frac{d\theta_{cond}}{dt}\right] \tag{45}$$

Rearranging Eq. (42) yields the liquid rewetting velocity

$$U_r = \frac{d\varepsilon}{dt} = U + \frac{2kA_sD(L - \varepsilon + L_c)}{\rho_l A_l h_{fg}} \tag{46}$$

where ε and D are obtained by numerically integrating the set of Eqs. (45) and (46). The temperature profile and rewetting

velocity then are obtained from Eqs. (44) and (46), respectively.

Results

Brennan et al.[9] presented experimental results for the startup process of two axially grooved oxygen–aluminum heat pipes, referred to as the TRW heat pipe and the Hughes heat pipe. The two heat pipes were flown onboard STS-53 in December 1992 as part of the CRYOHP flight experiment, and were mounted and flown as a Hitchhiker canister experiment. Several platinum-RTDs were utilized per heat pipe for axial wall temperature measurements. Each heat pipe condenser section was cooled using a Stirling cycle cryocooler. The primary dimensions and parameters as presented by Brennan et al.[9] for the two heat pipes are given in Table 1. As part of the CRYOHP experiment, several startup cycles were performed for each heat pipe, both in microgravity and ground environments. Microgravity and 1 g data demonstrated that the startup process, and corresponding isothermalization, occurred more rapidly in ground tests. The decreased startup time in 1 g was attributed to the formation of a liquid puddle in the condenser region. The added hydrostatic height of the liquid puddle aids in the priming and rewetting of the heat-pipe wick structure. Therefore, as the current model does not include the effects of the added hydrostatic height, the comparison between the current model and experimental data was made using the microgravity data presented in Brennan et al.[9] In the current model, the condenser temperature was obtained by interpolating the experimental data at different time intervals, as the cryocooler head temperature was the dominant factor in setting the condenser temperature.

Table 1 Parameters for the TRW and Hughes heat pipes[9]

Parameter	TRW	Hughes
Outer diameter (mm)	11.2	15.91
Vapor diameter (mm)	7.37	8.64
Wall thickness (mm)	1.02	2.54
Length (m)		
Evaporator	0.15	0.15
Condenser	0.15	0.15
Transport section	1.32	1.37
Oxygen charge (g)	10.3	33.7
Number of grooves	17	27
Groove width (mm)	0.445	0.658
Wetted perimeter (mm)	2.09	3.25
Total groove area (mm^2)	6.07	23.2
Platinum–RTD location (m)		
Transport 1	0.15	0.39
Transport 2	0.72	0.87
Evaporator	1.17	1.22
Initial temperature (K)	280	285

The model was first compared with the TRW heat pipe, where the results of the analysis and the corresponding data are shown in Fig. 3. Four locations of temperature measurements were selected for comparison between the analytical model and experimental data. The selected axial locations are specified in Table 1 and include temperatures for the condenser, the evaporator, and two separate locations in the adiabatic, or transport, section, where the transport section temperatures are indicated by the corresponding axial location. Experimental data are represented symbolically, whereas predicted temperatures from the present model are represented by the corresponding curves. During the initial phase of the startup process, the condenser temperature remains above the critical point temperature of the oxygen working fluid (T_c = 154.8 K), and the heat transfer process only occurs by heat conduction. Additionally, in this initial period, the evaporator temperature remains constant and equal to the initial temperature. This indicates that the penetration depth associated with the

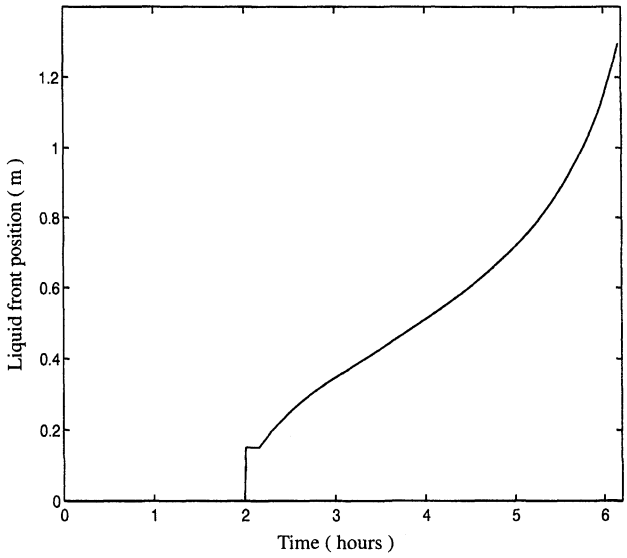

Fig. 4 Predicted liquid front position (TRW heat pipe).

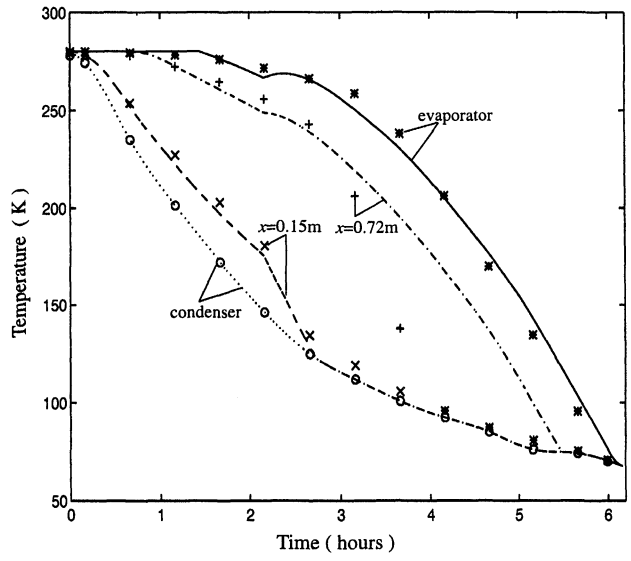

Fig. 3 Comparison between predicted and measured[9] temperatures (TRW heat pipe).

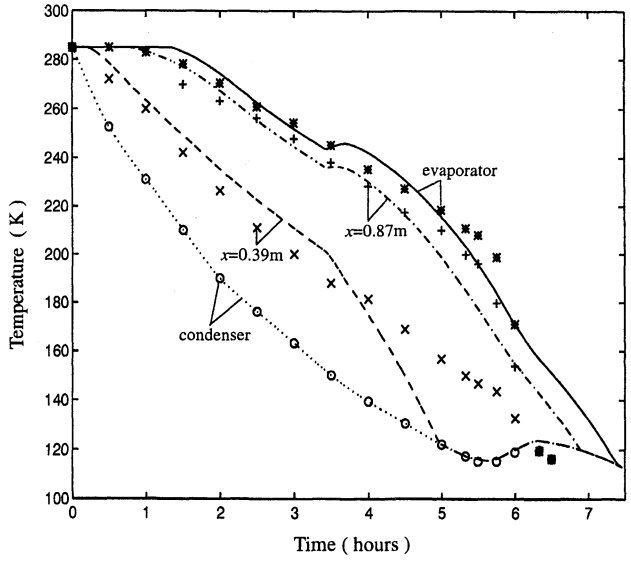

Fig. 5 Comparison between predicted and measured[9] temperatures (Hughes heat pipe).

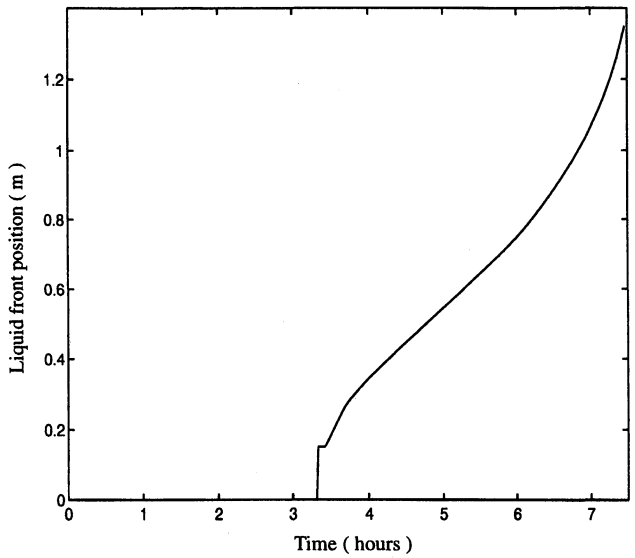

Fig. 6 Predicted liquid front position (Hughes heat pipe).

axial wall conduction has not yet reached the evaporator, as confirmed by the experimental data, i.e., the cooling effects in the condenser have not propagated over the entire length of the heat pipe. As seen, good overall agreement between the analytical model and the experimental data was found.

The formation and position of the liquid column in the grooves was analytically determined, where the location of the liquid front position for the TRW heat pipe is given in Fig. 4. As seen, for approximately the first 2 h following startup, no liquid was predicted to be present in the heat pipe. After approximately 2 h from startup, a liquid column was formed in the condenser, where it is interesting to note that even though the liquid column was established, the column was not predicted to immediately advance. The liquid column stagnation results from insufficient capillary pumping to overcome the high heat flux supplied to the leading edge of the liquid column by axial heat conduction. As the gradient of the temperature profile in the dry region is decreased over time, the liquid column begins to advance as the heat flux at the leading edge of the liquid column correspondingly decreases. Additionally, as the penetration depth in the dry region reaches the evaporator end of the heat pipe, the rewetting process accelerates and the liquid column advances more rapidly. Similar results were found with the data and model comparison for the Hughes heat pipe presented in Figs. 5 and 6.

Conclusions

An integral method was used to study the startup process of axially grooved cryogenic heat pipes from the supercritical state. The supercritical startup model incorporates hydrodynamic and conduction effects within the cryogenic heat pipe. The model presented is an easily integrated system of equations, does not require numerical code development nor utilization, and provides insight into the startup behavior and characteristics for the given systems. Using the developed model, the rewetting velocity, transient temperature distribution, and liquid front position were obtained. The theoretical analysis and experimental microgravity data for two oxygen–aluminum heat pipes were found to be in good agreement.

References

[1]Chang, W. S., "Heat Pipe Startup from the Supercritical State," Ph.D. Dissertation, Georgia Inst. of Technology, Atlanta, GA, 1981.

[2]Rosenfeld, J. H., Wolf, D. A., Buchko, M. T., and Brennan, P. J., "A Supercritical Start-Up Limit to Cryogenic Heat Pipes in Microgravity," *Proceedings of the 9th International Heat Pipe Conference* (Albuquerque, NM), Vol. II, Los Alamos National Lab., Los Alamos, NM, 1995, pp. 742–753.

[3]Ochterbeck, J. M., Peterson, G. P., and Ungar, U. K., "Depriming/Rewetting of Arterial Heat Pipes: Comparison with SHARE-II Flight Experiment," *Journal of Thermophysics and Heat Transfer*, Vol. 9, No. 1, 1995, pp. 101–108.

[4]Peng, X. F., and Peterson, G. P., "Analysis of Rewetting for Surface Tension Induced Flow," *Journal of Heat Transfer*, Vol. 114, No. 3, 1992, pp. 703–707.

[5]Yan, Y. H., and Ochterbeck, J. M., "Integral Method Solutions for Rewetting of Finite Length Surfaces with Uniform Heating," AIAA Paper 96-3975, Aug. 1996.

[6]Scott, R. B., *Cryogenic Engineering*, Van Nostrand, Inc., Princeton, NJ, 1959.

[7]Van Wylen, G., Sonntag, R., and Borgnakke, C., *Fundamentals of Classical Thermodynamics*, 4th ed., John Wylen & Sons, Inc., New York, 1993.

[8]Chi, S. W., *Heat Pipe Theory and Practice: A Sourcebook*, Hemisphere, Washington, DC, 1976.

[9]Brennan, P. J., Thienel, L., Swanson, T., and Morgan, M., "Flight Data for the Cryogenic Heat Pipe (CRYOHP) Experiment," AIAA Paper 93-2735, July 1993.